THE JOURNAL OF BIOLOGICAL CHEMISTRY VOL. 288, NO. 4, pp. 2475–2484, January 25, 2013

Four of the Most Common Mutations in Primary Hyperoxaluria Type 1 Unmask the Cryptic Mitochondrial Targeting Sequence of Alanine:glyoxylate Aminotransferase Encoded by the Polymorphic Minor Allele*

Received for publication, October 31, 2012, and in revised form, December 3, 2012 Published, JBC Papers in Press, December 10, 2012, DOI 10.1074/jbc.M112.432617

Sonia Fargue[‡], Jackie Lewin[§], Gill Rumsby[¶], and Christopher J. Danpure[‡1]

From the [‡]Department of Cell and Developmental Biology, University College London, London WC1E 6BT, United Kingdom, the [§]Electron Microscopy Unit, Royal Free and University College Medical School, London NW3 2PF, United Kingdom, and the [¶]Department of Clinical Biochemistry, University College London Hospitals, London W1T 4EU, United Kingdom

Background: The hereditary kidney stone disease primary hyperoxaluria type 1 (PH1) is caused by a deficiency of the peroxisomal enzyme alanine:glyoxylate aminotransferase (AGT).
Results: Four mutations interact with a common polymorphism resulting in AGT mitochondrial mistargeting.
Conclusion: The synergy between the polymorphism and mutations in AGT is more common than thought previously.
Significance: This has implications for the design of chemotherapeutic agents.

The gene encoding the liver-specific peroxisomal enzyme alanine:glyoxylate aminotransferase (AGT, EC. 2.6.1.44) exists as two common polymorphic variants termed the "major" and "minor" alleles. The P11L amino acid replacement encoded by the minor allele creates a hidden N-terminal mitochondrial targeting sequence, the unmasking of which occurs in the hereditary calcium oxalate kidney stone disease primary hyperoxaluria type 1 (PH1). This unmasking is due to the additional presence of a common disease-specific G170R mutation, which is encoded by about one third of PH1 alleles. The P11L and G170R replacements interact synergistically to reroute AGT to the mitochondria where it cannot fulfill its metabolic role (*i.e.* glyoxylate detoxification) effectively. In the present study, we have reinvestigated the consequences of the interaction between P11L and G170R in stably transformed CHO cells and have studied for the first time whether a similar synergism exists between P11L and three other mutations that segregate with the minor allele (*i.e.* I244T, F152I, and G41R). Our investigations show that the latter three mutants are all able to unmask the cryptic P11L-generated mitochondrial targeting sequence and, as a result, all are mistargeted to the mitochondria. However, whereas the G170R, I244T, and F152I mutants are able to form dimers and are catalytically active, the G41R mutant aggregates and is inactive. These studies open up the possibility that all PH1 mutations, which segregate with the minor allele, might also lead to the peroxisome-to-mitochondrion mistargeting of AGT, a suggestion that has important implications for the development of treatment strategies for PH1.

In European and North American populations, 15–20% of the alleles encoding the liver-specific peroxisomal enzyme alanine:glyoxylate aminotransferase (AGT,[2] EC 2.6.1.44) encode a cryptic N-terminal mitochondrial targeting sequence (MTS) (1, 2). The polypeptide encoded by this allele, termed the "minor allele," differs from that encoded by the more common "major allele," most importantly by the presence of a P11L amino acid replacement, which generates an optimal motif for binding to the mitochondrial import receptor TOM20 (1, 3–5). However, the P11L-generated MTS is functionally ineffective because the N-terminal extension in which it is located is tightly bound to the surface of the neighboring subunit in the fully folded dimeric protein (6). Not only is the TOM20 interaction motif masked but also the high stability of the AGT dimer generates a conformation incompatible with mitochondrial import (7, 8). The resulting functional inefficiency of this cryptic MTS means that only a very small proportion (~5%) of AGT encoded by the minor allele finds its way to the mitochondria (1). Despite being masked, the intrinsic strength of this unusual noncleavable MTS is shown by the observations that when the AGT folding/dimerization pathways are disrupted, for example by increasing the temperature or by targeted amino acid replacements, or if the N-terminal 20 amino acids encoded by the minor allele are attached to a reporter protein, the resulting construct is rapidly imported into mitochondria (9, 10). Exposure of this cryptic MTS can have very serious consequences, as is the case for a subset of patients with the hereditary calcium oxalate kidney stone disease primary hyperoxaluria type 1 (PH1, OMIM 259900) (1, 11, 12). In these patients, the synergistic interaction between the P11L amino acid replacement characteristic of the minor allele and a disease-specific G170R mutation increases the efficiency of the P11L-generated MTS so that the great majority (~90%) of the enzyme is rerouted to the mitochondria (1, 2, 8, 11, 13).

* This work was supported by grants from the Oxalosis and Hyperoxaluria Foundation (to C. J. D.) and the Société Française de Néphrologie (to S. F.).
[1] To whom correspondence should be addressed: Dept. of Cell and Developmental Biology, Div. of Biosciences, University College London, Gower Street, London WC1E 6BT, UK. Tel.: 44-0-207-679-7936; E-mail: c.danpure@ucl.ac.uk.

[2] The abbreviations used are: AGT, alanine:glyoxylate aminotransferase; PH1, primary hyperoxaluria type 1; GO, glycolate oxidase; BS(PEG)$_5$, bis-*N*-succinimidyl-(pentaethyleneglycol) ester; MW, molecular weight; PLP, pyridoxal-5′-phosphate.

TABLE 1

Properties of normal and mutant forms of AGT used in the present study

M/m, major/minor mitochondrial localization; P/p, major/minor peroxisomal localization. Information was from multiple sources (9, 16–18, 21–23, 25, 34, 47–50).

AGT construct	Amino acid changes compared with AGT-MA	Enzyme activity compared with AGT-MA (%)		Intracellular localization	
		Recombinant protein	Liver	Transfected COS cells	Liver[a]
AGT-MA[b]		100	100	P	P
AGT-mi[c]	P11L, I340M	45–100	90	P	P + m
AGT-anc[d]	$^{-22}$MFQALAKASAAPGSRAAGWVRT^{-1}			M + p	M + p
AGT-41[e]	P11L, G41R, I340M	<10–24	0		p[f]
AGT-152[e]	P11L, F152I, I340M	<10–80	0–16		m + p[g]
AGT-170[e]	P11L, G170R, I340M	<10–76	10–72	M + p	M + p
AGT-244[e]	P11L, I244T, I340M	<10–26	0–36	P	

[a] Human liver except for AGT-anc where the distribution has been determined in marmoset liver.
[b] Normal AGT encoded by the major allele.
[c] Normal AGT encoded by the minor allele
[d] Cleavable ancestral (marmoset) 22-amino acid leader sequence added to the N terminus of AGT-MA.
[e] Mutant AGTs found in PH1 all on the background of the minor allele.
[f] Peroxisomal cores as extrapolated from a compound AGT-41/AGT-152 compound heterozygote.
[g] Distribution extrapolated from a compound AGT-41/AGT-152 compound heterozygote.

Although mistargeted AGT remains catalytically active in the mitochondria, it is metabolically inefficient. This is because most of its substrate (*i.e.* glyoxylate) in synthesized in the peroxisomes. Failure to transaminate glyoxylate to glycine within the peroxisomes, allows glyoxylate to diffuse into the cytosol where it is oxidized to the metabolic end product oxalate, catalyzed by lactate dehydrogenase (14). It is this elevated synthesis of oxalate that leads to all of the pathological sequelae of PH1, most notably the progressive deposition of insoluble calcium oxalate in the kidney and urinary tract (12).

As most of the missense mutations in AGT that cause PH1 segregate with the minor allele, it is of considerable interest to know whether synergistic interactions, including peroxisome-to-mitochondrion mistargeting, occur between these mutations and the P11L polymorphism. Little information is currently available about the intracellular compartmentalization of other mutant forms of AGT either *in situ* (*i.e.* in the liver) or in tissue culture cell lines. That which is available shows that a G82E mutant form of AGT segregating with the major allele is peroxisomal in human liver (15). In addition, an I244T mutant on the background of the minor allele is also peroxisomal in transiently transfected COS cells (16). The liver of a compound heterozygote PH1 patient (F152I and G41R, both on the minor allele) had both peroxisomal and mitochondrial AGT (17). However, in the latter case, overall expression was very low so that the distribution profile could easily have been distorted. Therefore, it is not clear whether such synergistic interactions, including AGT mistargeting, does actually occur with other mutations. Previous studies on recombinant AGT expressed in *Escherichia coli* suggests that P11L and all other minor allele mutations studied (*i.e.* G170R, I244T, F152I, and G41R) do interact synergistically, at least in terms of protein stability (18–21); but, whether this is paralleled by mistargeting in a eukaryotic system, is unknown. To investigate this, we have explored the intracellular compartmentalization, oligomeric status, and enzyme activity of three common mutant forms of AGT encoded by the minor allele in stably transformed CHO cells and compared the results with those found for the previously studied G170R mutant.

We show that three other disease-causing mutations, in addition to G170R, (*i.e.* I244T, F152I, and G41R), with all four representing ~40% of PH1 alleles (16, 22–25), can functionally unmask the cryptic MTS generated by the P11L polymorphism characteristic of the minor allele. This opens up the possibility that all missense mutations that co-segregate with this allele might lead to the peroxisome-to-mitochondrion mistargeting of AGT. As this would account for half of all mutant alleles, this finding has considerable importance for the development of treatment strategies for PH1. In addition, we show that three of the four mutations that lead to AGT mistargeting do not prevent AGT dimerization or the acquisition of at least some catalytic activity in stably transformed CHO cells.

EXPERIMENTAL PROCEDURES

Expression Constructs and Cell Lines—The full-length cDNAs of AGT and glycolate oxidase (GO) were subcloned in the mammalian expression vectors pcDNA3.1(+)neo and pcDNA3.1(−)zeo, respectively (both from Invitrogen). The different AGT constructs used in this study are described in Table 1. AGT-MA, AGT-mi, AGT-anc, AGT-170, AGT-152, and AGT-41 were prepared as described previously (10, 18, 26, 27). All of the AGT constructs except AGT-MA and AGT-244 already existed and were recloned from a pHYK vector into pcDNA3.1. AGT-244 was created by site-directed mutagenesis and cloned into pcDNA3.1.

CHO cell lines expressing AGT variants were established by retransforming a CHO cell line previously transformed with GO and created for other purposes not described (27). Three cell lines expressed normal AGT variants: AGT-MA expressing AGT encoded by the major allele of *AGXT*, with AGT-mi expressing AGT encoded by the minor allele of *AGXT*, and AGT-anc expressing a variant of AGT-MA to which a more usual cleavable N-terminal MTS was added, similar to marmoset AGT (28). Four cell lines expressing mutant AGTs were used: AGT-170, AGT-152, AGT-244, and AGT-41.

Cell Culture and Transformation—All GO and AGT double-transformed cell lines were created from one single CHO GO cell line retransformed with AGT constructs following the methods published previously (27) with the difference that cells were transfected with Turbofect (Fermentas). CHO cells were cultured in Ham's F12 medium supplemented with 10% fetal calf serum and the addition of zeocin (400 μg/ml, Invitrogen)

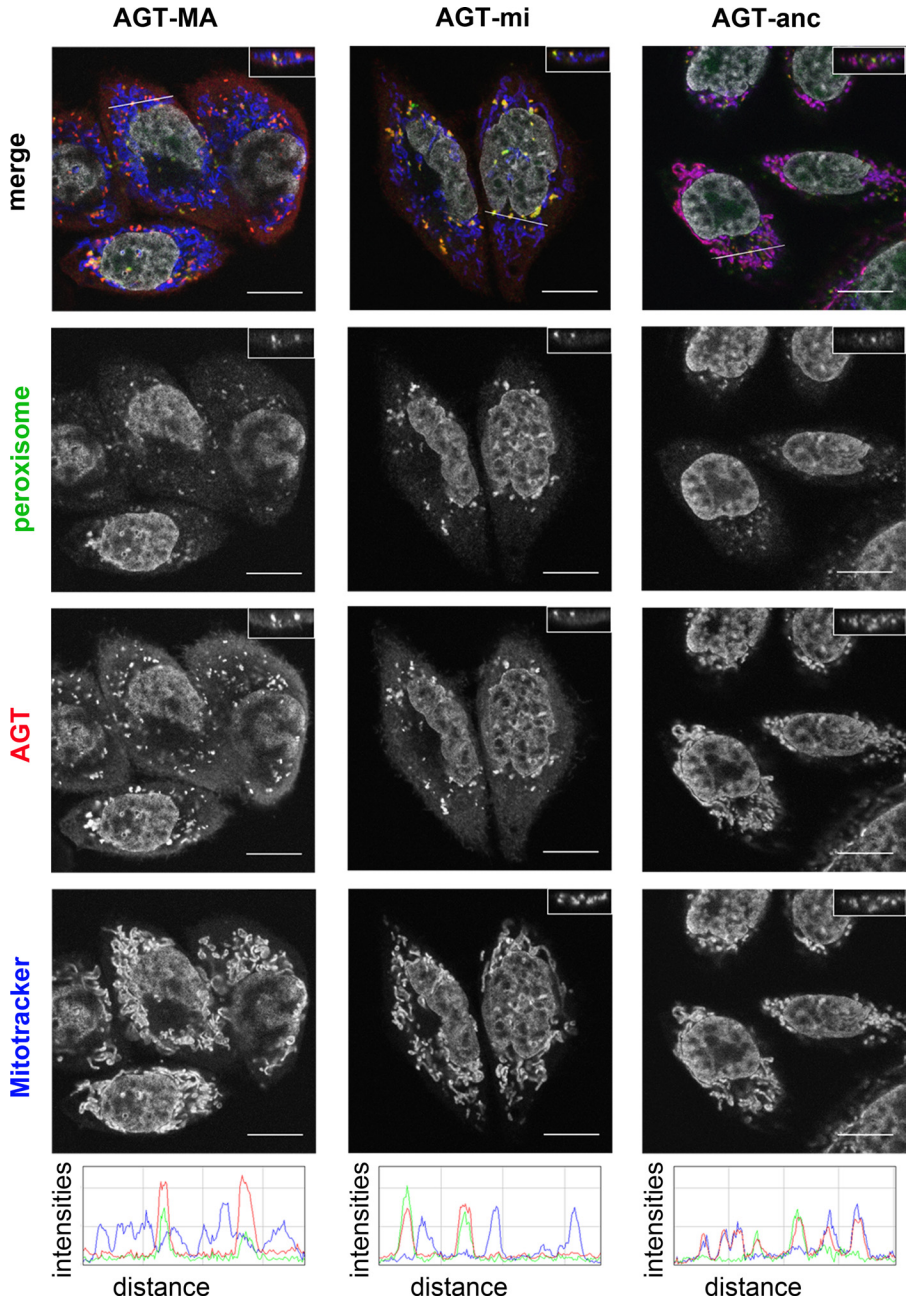

FIGURE 1. **Subcellular distribution of various normal AGT constructs in stably transformed CHO cells as shown by immunofluorescence microscopy.** Cells were stained with anti-peroxisomal proteins (*green*), anti-AGT (*red*), and MitoTracker (*blue*). Nuclei were stained with Hoechst (*gray*). *Scale bars*, 10 μm. Merged and single channel images from a single z-plane are shown for cells expressing AGT-MA, AGT-mi, and AGT-anc. *Insets*, reslice along the *z* axis along the line drawn in the merged image. *Below* is shown the *red*/*green*/*blue* (RGB) profile plotted along the line drawn in the merged image: *blue line*, mitochondria (MitoTracker); *green line*, peroxisomes (anti-peroxisomal proteins); *red line*, AGT (anti-AGT).

and G418 (800 μg/ml, Invitrogen) for the selection maintenance of GO and AGT, respectively, as described previously (27). The levels of expression of AGT in the cell lines remained stable over a period of at least 3 months, with at least 95% of cells expressing AGT.

Immunofluorescence Microscopy and Image Analysis—Cells on 13-mm glass coverslips were prepared for immunofluorescence microscopy and stained as described previously with various combinations of rabbit or guinea pig polyclonal anti-human AGT, anti-rat liver peroxisomal proteins, and MitoTracker (Red, CMXRos, Molecular Probes, Invitrogen) (27, 29). The image acquisition was carried out using a confocal laser-scanning fluorescence microscope (Leica TCS SPE), and the image analysis was carried out using ImageJ software (National Institutes of Health, Bethesda, MD). For quantitative colocalization analysis, Manders' and Pearson's coefficients were calculated using the ImageJ JACoP plugin (30) with manually set thresholds.

Immunoelectron Microscopy—Immnuoelectron microscopy on cells was carried out as published previously (17, 29). Briefly, fixed cells were stained with polyclonal rabbit anti-human AGT antiserum and then with 10-nm colloidal gold conjugated to anti-rabbit IgG.

Immunoblotting and Chemical Cross-linking—Cell lysates were analyzed by SDS-PAGE and immunoblotting following a

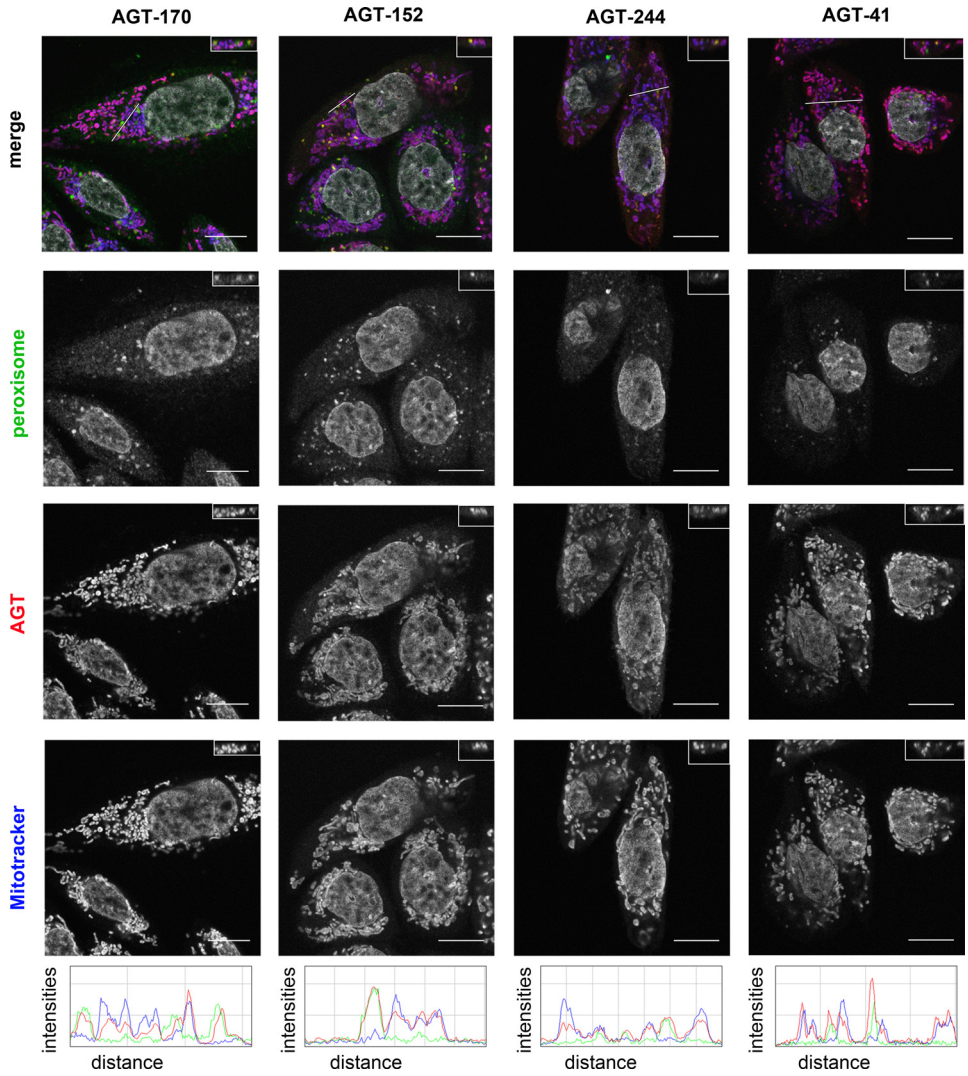

FIGURE 2. **Subcellular distribution of various PH1 mutant AGT constructs, in stably transformed CHO cells as shown by immunofluorescence microscopy.** Cells were stained with anti-peroxisomal proteins (*green*), anti-AGT (*red*), and MitoTracker (*blue*). Nuclei were stained with Hoechst (*gray*). *Scale bars*, 10 μm. Merged and single channel images from a single z-plane are shown for cells expressing AGT-170, AGT-152, AGT-244, and AGT-41. *Insets*, reslice along the *z* axis along the line drawn in the merged image. Below is shown the RGB profile plotted along the line drawn in the merged image: *blue line*, mitochondria (MitoTracker); *green line*, peroxisomes (anti-peroxisomal proteins); *red line*, AGT (anti-AGT).

previously described method (27, 29). Chemical cross-linking was carried out using bis-*N*-succinimidyl-(pentaethyleneglycol) ester, (BS(PEG)$_5$, Pierce) as described previously (29). For densitometry analysis of Western blots, the chemiluminescent signal was recorded from the membrane with a camera (ImageQuant LAS 4000). The file was then analyzed using the measure tool in ImageJ software (NIH). Results were expressed relative to the densitometry of AGT-MA in each gel analyzed.

Catalytic Activity—AGT activities in cell lysates were measured as published previously by a spectrophotometric method (27, 31).

RESULTS

All PH1 Mutations Studied Functionally Unmask the Cryptic MTS of AGT Encoded by the Minor Allele (i.e. AGT-mi)—To investigate whether other disease-causing mutations that segregate with the minor AGT allele lead to peroxisome-to-mitochondrion AGT mistargeting, the intracellular compartmentalization of various normal and mutant AGT constructs has been studied in stably transformed CHO cells. Immunofluorescence microscopic analysis of these cells is shown in Figs. 1–3. As has been shown before in transiently transfected COS cells (9) and microinjected human fibroblasts (13), AGT-MA and AGT-mi were peroxisomal (Fig. 1), whereas AGT-anc (Fig. 1) and AGT-170 (Fig. 2) were predominantly mitochondrial with a minority peroxisomal. Qualitative (Fig. 2) and quantitative (Fig. 3) analysis indicated that AGT-152, similar to AGT-170 and AGT-anc, was mainly mitochondrial with a minority peroxisomal. On the other hand, AGT-244 and AGT-41 were shown to be more evenly distributed between mitochondria and peroxisomes.

Higher resolution analysis of the distribution of the constructs by immunoelectron microscopy (Fig. 4) confirmed the mitochondrial and peroxisomal localization of AGT-anc, AGT-170, AGT-152, AGT-244, and AGT-41. In addition, it was able to detect a small amount of mitochondrial AGT-mi,

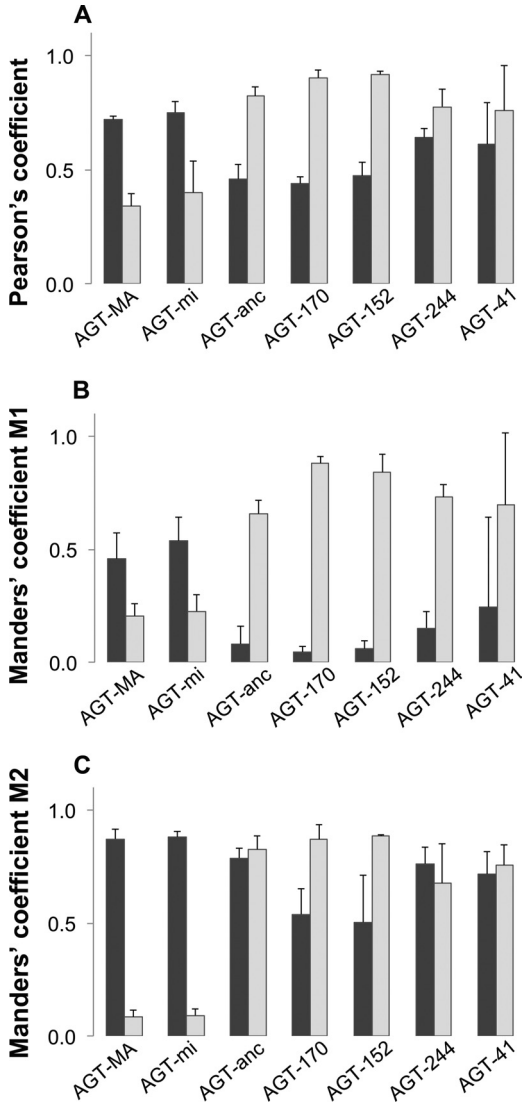

FIGURE 3. **Immunofluorescence microscopy colocalization coefficients for the subcellular distribution of AGT variants in stably transformed CHO cells.** *A*, Pearson's colocalization coefficient, calculated for the colocalization of AGT and peroxisomes (*dark gray*) and for AGT and mitochondria (*pale gray*); *B*, Manders' M1 coefficients for the colocalization AGT with the peroxisomal marker (*dark gray*) and for AGT with mitochondrial marker (*pale gray*); *C*, Manders' M2 coefficients for the colocalization peroxisomal marker with AGT (*dark gray*) and for mitochondrial marker with AGT (*pale gray*). Coefficients were calculated using the ImageJ JACoP plugin, with manual thresholding, on image stacks of cells stained concomitantly with anti-AGT, anti-peroxisomes, and MitoTracker. The results are given as means (+ S.D.) of several images; at least 10 individual cells were analyzed for each coefficient.

which was not noticeable by immunofluorescence microscopy. In the case of AGT-41, the peroxisomes contained large amorphous "cores," not present with the other constructs (Fig. 4*B*). These cores stained for AGT and at least one other peroxisomal enzyme GO (data not shown).

Mutant AGTs on the Background of the Minor Allele Can Still Dimerize—Previous studies have shown that the peroxisome-to-mitochondrion mistargeting of AGT is accompanied by a decrease in the rate of dimerization but not its abolition (8, 9). In fact, this interference with dimerization has been suggested to be an integral part of the mistargeting process (8). To determine whether mutations that cause AGT mistargeting affect the steady state dimeric status of AGT in transformed CHO cells, the expression of normal and mutant AGT variants has been investigated by SDS-PAGE and immunoblotting.

All AGT constructs showed a prominent band of ~43 kDa, the expected size of the monomer (Fig. 5*A*). Surprisingly, however, for a denaturing gel, minor bands of 80–90 kDa were also present for many of the constructs. This is compatible with the size expected for the dimer. In addition, to strong bands in the region of 80–90 kDa, cells expressing AGT-41 showed many other high molecular weight (MW) bands. Altogether, these high MW bands in AGT-41 were much more prominent than the 43-kDa band of the monomer. Cells expressing AGT-anc exhibited an additional monomeric band of ~45 kDa, presumably representing the preprotein (most likely peroxisomal), which still retains the ancestral cleavable MTS leader sequence. Cells expressing the mutant AGT constructs also show variable amounts of a lower MW band of ~38–40 kDa. This was most noticeable in cells expressing AGT-41. These lower MW bands disappeared when the blot was incubated with antibodies raised against the N terminus of AGT (data not shown), suggesting that they resulted from N-terminal clipping.

When cells were incubated with the bifunctional cross-linker $BS(PEG)_5$, strong bands of 80–90 kDa were very prominent, indicating that in all cases, dimerization had occurred (Fig. 5*B*). Although monomeric bands were also present after cross-linking, they disappeared when the concentration of the cross-linker was increased (data not shown). The double dimeric bands, which also formed when purified recombinant AGT was cross-linked (Fig. 5*C*), presumably represent structural isoforms separated by the SDS-PAGE. Heavy staining of the immunoblot in Fig. 5*B* showed the additional presence of high MW cross-linked bands in many of the normal and mutant AGT constructs, presumably due to the presence of higher order multimers. Many of the high MW bands found in cells expressing AGT-41 (Fig. 5*A*) disappeared after cross-linking (Fig. 5, *B* and *C*), probably due to the formation of very high MW structures unable to enter the gel matrix.

AGT-41, but Not the Other Mutant Constructs, Aggregates Intraperoxisomally—Because missense mutations in protein-encoding genes often lead to the instability and subsequent aggregation of the encoded proteins and because immunoelectron microscopy showed that AGT-41 formed intraperoxisomal aggregates (see above), the presence of such was investigated in the present system by pelleting cell lysates with low speed centrifugation (600 × *g* for 10 min). The supernatants and pellets were analyzed by SDS-PAGE and immunoblotting (Fig. 6). Whereas almost all of the normal and mutant AGT constructs remained in the supernatant, more than half of the AGT-41, including most of the higher MW bands, came down in the pellet. Therefore, apart from AGT-41, macroaggregation intracellular did not seem to occur with normal or mutant AGT.

Except for AGT-41, the Mutant Forms of AGT on the Background of the Minor Allele Retain at Least Some Functional (i.e. Catalytic) Activity—One of the best surrogates for determining the extent to which an enzyme has attained the correct structural conformation intracellularly is to determine its catalytic activity. The assays were carried out on whole cell lysates in the

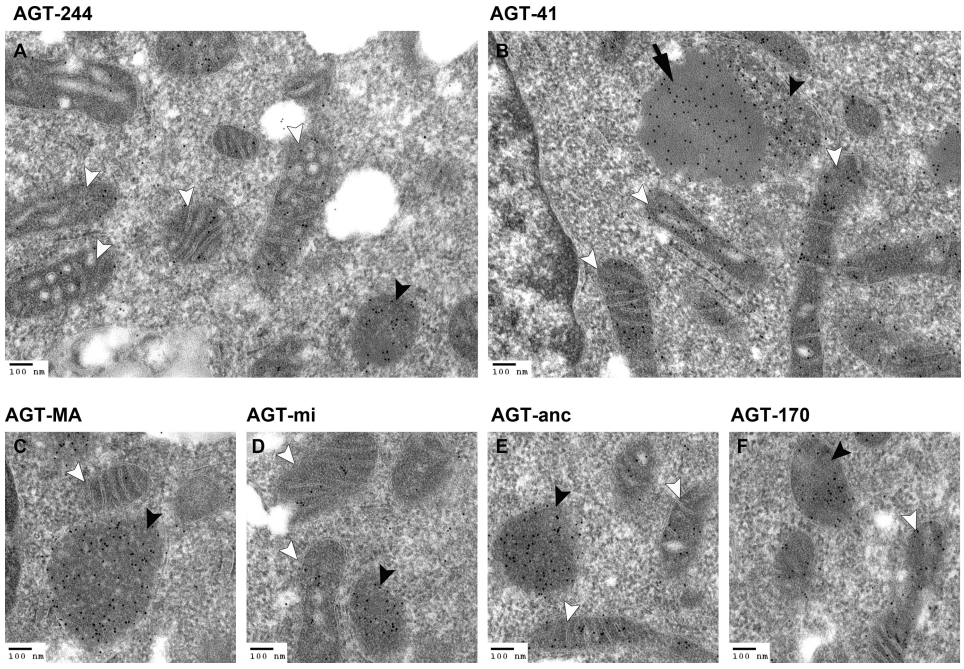

FIGURE 4. **Subcellular distribution of various normal and mutant AGT constructs in stably transformed CHO cells as shown by immunoelectron microscopy.** Cells expressing various forms of AGT (*A*, AGT-244; *B*, AGT-41; *C*, AGT-MA; *D*, AGT-mi; *E*, AGT-anc; *F*, AGT-170) were stained with anti-AGT and 10 nm of colloidal gold conjugated to anti IgG. *Scale bars*, 100 nm. *Black arrowheads*, peroxisomes; *white arrowheads*, mitochondria; *black arrow*, intraperoxisomal core (*B*). Data are not available for AGT-152.

presence and absence of the cofactor pyridoxal-5′-phosphate (PLP) to determine the level of holo-AGT (activity in the absence of PLP in the assay) and apo-AGT (difference between the activities in the presence and absence of PLP in the assay). The results in Table 2 show that, with the exception of AGT-41, all normal and mutant constructs were catalytically active in stably transformed CHO cells. Cells expressing AGT-41 showed no activity. In the presence of PLP, the activities ranked as follows: AGT-MA > AGT-mi = AGT-anc > AGT-170 > AGT-152 = AGT-244 ≫ AGT-41. All of the mutants had activities significantly lower than the normal AGTs. Interestingly, the differences between the activities in the presence and absence of PLP were negligible, except for AGT-152, suggesting that in most cases, the AGT was present mainly as the holo protein. AGT-152, on the other hand, seemed to be present entirely as the apo protein. Densitometric scans of the immunoblots (Table 2) indicated that at least some of the differences in AGT activity could be attributed to different levels of net expression.

DISCUSSION

The peroxisome-to-mitochondrion mistargeting of AGT is unparalleled in human genetic disease. Although previously thought to be restricted to G170R on the background of the minor allele, the present studies open up the possibility that all, or at least most, of the mutations segregating on the minor allele might also lead to mistargeting. As the frequency of the minor allele is ~50% in PH1 patients, compared with 15–20% in the general population (32), it suggests that AGT mistargeting in PH1 might be much more common than previously thought.

Previous studies of the peroxisome-to-mitochondrial mistargeting of PH1 mutant AGT with the G170R amino acid replacement on the background of the minor allele showed that the P11L polymorphism was entirely responsible for providing the mitochondrial targeting information (1, 2). The exact role of the G170R mutation was unclear as it had relatively little effect on the conformation and other properties of AGT on its own (8, 18, 20, 33). However, it did appear to interact synergistically with the P11L polymorphism to interfere with AGT dimerization and possibly freeing up the otherwise trapped N-terminal extension (8, 9). Whether the latter was a cause or a result of interference of dimerization was unclear. In any case, the present study shows that the steady state of most of the AGTs containing mutations which lead to mistargeting is dimeric, as it is for normal AGTs. In addition, the presence of enzyme activity suggests that these dimers are structurally relatively normal, at least in terms of the active site environment. The only exception is AGT-41, which appears to exist in multiple polymeric states and aggregates. Therefore, it is likely that all mutations studied slow down the process of folding and/or dimerization, rather than preventing it. This would allow the still free N-terminal polymorphic MTS more time to interact with its binding site on TOM20.

At a structural level, it is clear that the N-terminal extension, which contains the P11L amino acid replacement of the minor allele, plays no direct part in the catalytic activity of AGT (6). So its role is unclear, although it has been suggested that it might initiate, or at least aid, the dimerization process (8, 9). This suggestion has been reinforced by the finding that mutations that interfere with the interaction of this extension and the surface of the neighboring subunit, do indeed inhibit dimerization *in vitro* translations (9). But the N-terminal extension of AGT is clearly not essential for dimerization, as its removal still allows AGT to form dimers, albeit inactive and probably con-

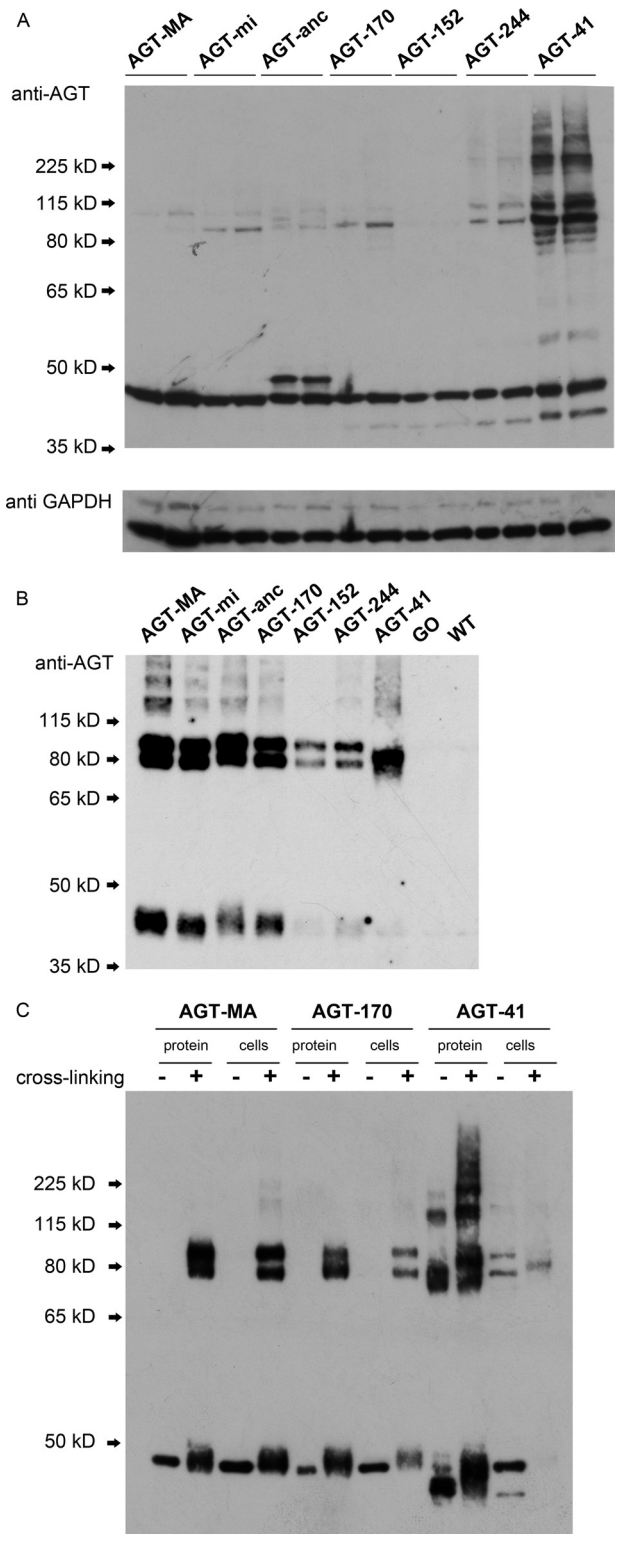

FIGURE 5. **Expression and dimerization status of AGT variants in stable CHO transformants shown by immunoblotting.** Whole cell lysates were electrophoresed by SDS-PAGE and blotted onto nitrocellulose membranes, which were then incubated with anti human-AGT (*A–C*) and with anti GAPDH for loading control (*A*). *A*, noncross-linked cell lysates (each lane was loaded in duplicate with 5 μg of total cell protein); *B*, cell lysates cross-linked with $BS(PEG)_5$ at 1250 μM (each lane was loaded with 2 μg of total cell protein); *C*, cell lysates (cells) and purified recombinant AGT expressed in *E. coli* (protein) were cross-linked with $BS(PEG)_5$ at 1250 μM (+) or not cross-linked (−). For cell samples, 6 μg of protein were loaded per lane, for purified AGT 50 ng were loaded. The purified recombinant AGT was a kind gift from Dr Cellini (University of Verona). *kD*, kDa.

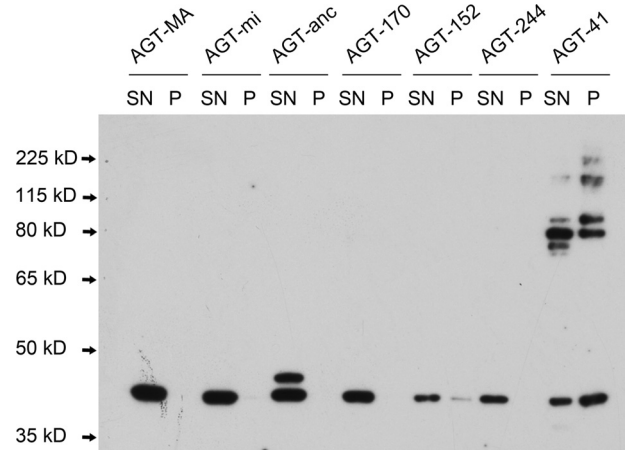

FIGURE 6. **Presence or absence of aggregates in CHO cell lines stably expressing normal and mutant AGT constructs.** Whole cell extracts of CHO cells stably expressing AGT variants were centrifuged at 600 × *g* for 10 min, and the resulting supernatant (*SN*) and pellet (*P*) were immunoblotted against anti-AGT. Each *lane* was loaded with 5 μg of total cell protein.

formationally abnormal, both in cells (the present study) and in purified recombinant protein (29).

There are no structures available for any AGT mutant, except the isolated G170R mutant, so that it is unknown whether the additional mutations studied here have any significant effects on their own (*i.e.* in the absence of the P11L replacement). Previous studies on purified recombinant AGT expressed in *E. coli* suggest that, except for G41R, they do not (18, 21, 34). Therefore it is likely that peroxisome-to-mitochondrion mistargeting caused by these mutations, all result from a similar synergistic interaction to that previously identified for G170R. A dual localization of proteins is known for a number of proteins, sometimes both peroxisomal and mitochondrial (35–37). The role and speed of protein folding in the final distribution of a partly mitochondrial protein has been shown for some enzymes such as fumarase (38, 39) and yeast major adenylate kinase (40). Such a mechanism could also control the abnormal dual targeting of AGT mutants in PH1 patients.

The mutant forms of AGT in this study are all predicted, or have been shown, to lead to AGT instability (16, 18, 21, 34, 41), although the consequences for their intracellular behavior were less certain. The present study suggests that any mutation on the minor allele that leads to protein instability and/or interferes with the process of folding or dimerization could lead to peroxisome-to-mitochondrion mistargeting directed by the P11L-generated MTS. The final destination of minor allele mutant AGTs is dependent on kinetic partitioning of the newly synthesized polypeptide in the cytosol between folding, dimerization, mitochondrial import, peroxisomal import, aggregation, and proteolysis (see Fig. 7). So that the slower the folding and dimerization is, the greater will be the mistargeting to the mitochondria. It is possible that if the acquisition of the correct conformation is delayed for too long, aggregation and proteolysis will then predominate. Interestingly, only AGT-41 showed any propensity to aggregate when expressed in stably transformed CHO cells, although other mutants studied here (*i.e.* AGT-244 and AGT-152) tended to aggregate in other systems (*i.e.* transiently transfected COS cells and purified recom-

TABLE 2
AGT catalytic activities in stably transformed CHO cell lines

AGT construct	*n*	AGT activity[a]			Net AGT expression[b]
		−PLP	+PLP	−PLP/+PLP	
AGT-MA	8	41.7 ± 7.1	44.6 ± 11.4**	0.96 ± 0.18	1.00
AGT-mi	8	28.4 ± 6.9	27.9 ± 5.2	1.05 ± 0.32	0.82 ± 0.33
AGT-anc	4	23.4 ± 3.1	25.0 ± 5.9	0.96 ± 0.14	1.18 ± 0.48
AGT-170	6	14.8 ± 4.2	14.2 ± 1.9***	1.06 ± 0.32	0.69 ± 0.31§
AGT-152	4	0.9 ± 1.7###	8.0 ± 0.9***	0.10 ± 0.18	0.34 ± 0.12§§§
AGT-244	4	7.0 ± 2.1	8.9 ± 2.2***	0.80 ± 0.21	0.56 ± 0.25§
AGT-41	4	0.6 ± 0.3	0.7 ± 0.2***	0.89 ± 0.38	2.16 ± 1.20
WT	6	0.7 ± 0.9	0.7 ± 0.5	1.00	

[a] The AGT assay was carried out in standard conditions without PLP (−PLP) or with 150 μmol/l PLP (+PLP). Units, μmol pyruvate/h/mg protein ± S.D., *n*, number of experiments for each construct. The limits of sensitivity of the AGT assay are 3 μmol pyruvate/h/mg protein. The reference range for AGT activity +PLP in human liver is 19.1–47.9 (26).

[b] For the net AGT expression, a densitometry analysis, including both monomer and oligomers, was performed on immunoblots loaded with the same amount of cell protein lysate for each cell line. The result is expressed as a ratio to that of the expression of AGT-MA in each immunoblot. Statistical significance was calculated using Student's *t* test. AGT activity +PLP was compared with that of AGT-mi (**, $p < 0.01$; ***, $p < 0.001$); AGT activity −PLP was compared with that of the same construct +PLP (###, $p < 0.001$); net AGT expression was compared with that of AGT-MA (§, $p < 0.05$; §§§, $p < 0.001$).

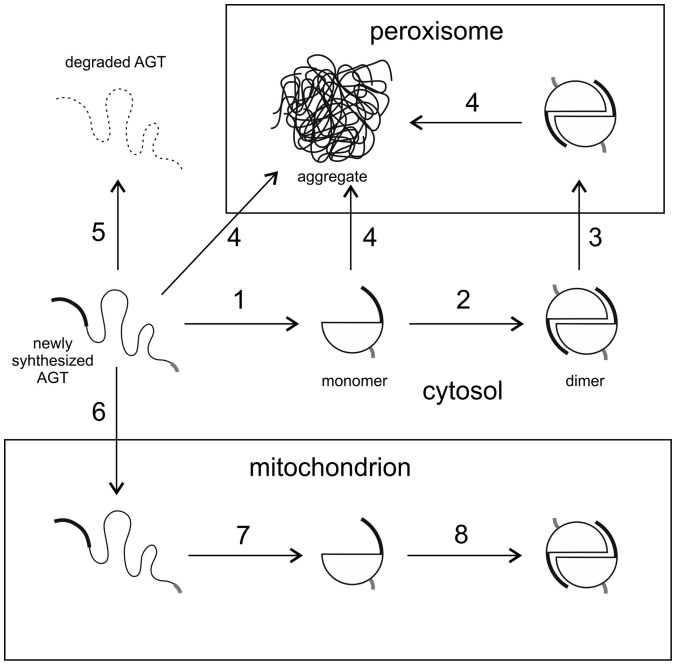

FIGURE 7. **Schematic representation of the intracellular kinetic partitioning of AGT-mi and its mutants.** Diagram shows the unfolded monomeric, folded monomeric, folded dimeric, aggregated and degraded forms of AGT-mi. The C-terminal type 1 peroxisomal targeting sequence (*thick gray line*) always remains available for interaction with the peroxisomal import receptor Pex5p and peroxisomal import, whereas the polymorphic N-terminal MTS (*thick black line*) is only available for interaction with the mitochondrial import receptor TOM20 and mitochondrial import in the unfolded monomeric species. AGT-MA is presumed to take mainly pathways 1→2→3 with rapid folding, dimerization, and peroxisomal import. Relatively little is expected to take pathway 5 (degradation). None will take pathway 6 (mitochondrial import) as AGT-MA does not contain a MTS. AGT-mi will be similar to AGT-MA, except that a small proportion (5–10%) will take pathway 6-7-8 due to the presence of the polymorphic MTS. The kinetics of AGT-mi folding and dimerization means that pathway 1→2→3 will predominate over pathway 6→7→8. As the net expression of AGT-mi tends to be lower than AGT-MA, some are expected to be degraded (5). AGT-mi mutants that destabilize the protein and slow down folding and/or dimerization (1→2) will increase both mitochondrial import (6) and the degradation (5). Most of the AGT-170 follows the mitochondrial pathway (6→7→8), with only a small proportion taking the peroxisomal pathway (1→2→3). Some will also be degraded (5). Most of AGT-152 is degraded (5), but the majority of the remainder will take the mitochondrial pathway (6→7→8). Most of AGT-244 is degraded (5), but the remainder is split between the peroxisomal (1→2→3) and mitochondrial (6→7→8) pathways. AGT-41 appears to be split between the peroxisomal (1→2→3) and mitochondrial (6→7→8) pathways. However, intraperoxisomal aggregation pathways (4) predominate. Although dimers form, they are likely to be highly abnormal as AGT-41 completely lacks catalytic activity. The intraperoxisomal aggregates might form in the peroxisome from any of the importable species (*i.e.* unfolded or folded monomers or folded dimer).

binant protein, respectively) (16, 34). Intriguingly, aggregates of AGT-41 were only found in peroxisomes and not in the cytosol or the mitochondria. Presumably, any aggregates formed in the cytosol would be degraded or imported into the peroxisomes, which are less fastidious about the conformational requirements for import (42). These aggregated species would be mitochondrially import incompetent, as only unfolded monomers can be imported (7). The folding environment inside mitochondria could be different enough from that in the cytosol or peroxisome to prevent aggregation.

All of the minor allele mutants in the present study showed N-terminal clipping to varying extents. This was especially noticeable for AGT-41 (see Fig. 5*A*). Previous studies using purified recombinant AGT-41 expressed in *E. coli* have shown that the N-terminal 40 or so amino acids are more flexible than the equivalent region in normal AGT (21). In fact, these authors suggest that this flexibility is at least partly responsible for the loss of catalytic activity of the mutant. This flexibility might occur in all minor allele mutants and, if so, could make available this region for N-terminal clipping by a nonspecific intracellular protease. Such an N-terminal clipping is different from the cleavage of the N terminus of AGT-anc, which is expected after mitochondrial import because AGT-anc contains a classical MTS and recognition sites for the mitochondrial processing peptidase.

Although the system of stably transformed CHO cells used in the present study is relatively simple, at least at the metabolic level, compared with liver cells, it has the advantage of being much more tractable. Except for enzyme activity, the information available on human PH1 liver is very limited. When compared with the information that is available in human liver and other systems, a number of similarities and differences are apparent. The ranking of enzyme activities found in stably transformed CHO cells, *i.e.* AGT-MA > AGT-mi > AGT-170 > AGT-152 = AGT-244 ≫ AGT-41 is similar to that in human liver, although in the latter case, the range between different patients is very large (see Table 1). The net levels of expression of immunoreactive protein for the AGT mutants in the livers of patients tend to be rather less than found in CHO cells. This is especially the case for AGT-41, which was expressed highly in CHO cells, but is very low in PH1 liver (at least in a compound F152I/G41R compound heterozygote)

(17). Such a difference may be due to the greater activity of the hepatocyte proteolytic machinery. No information is available regarding the intracellular compartmentalization of AGT-244 in PH1 liver. However, immunoelectron microscopy of a liver from a PH1 patient heterozygous for F152I and G41R showed a complex picture, some mitochondrial labeling and some peroxisomal labeling, notwithstanding the low overall labeling due to greatly reduced overall immunoreactivity (17). Most of the peroxisomal label was concentrated into cores, which family studies suggested was associated with the G41R mutation rather than the F152I mutation. Whether these intraperoxisomal cores are equivalent to the cores and aggregates found with AGT-41 in the present study is unclear.

The present system, essentially a steady state system, has similarities to other systems, as well as differences. For example, in transiently transfected COS cells, AGT-244 appears to be entirely peroxisomal and at least partially aggregated (16). This may be due to the different cells used or differences between transient and steady state expression. Our preliminary observations (not reported here) suggest that short term expression may favor peroxisomal rather than mitochondrial import of minor allele mutant AGTs and that the significantly different composition of the media (most notably pyridoxine concentration) in which COS and CHO cells are cultured could make a big difference in the way AGT folds, dimerizes and acquires functional activity.

The findings in the present study have important implications for the development of new strategies for the treatment of PH1, especially the search for chemotherapeutic agents that might counteract the effects of specific mutations. The potential of chemical chaperones as treatments has been established for other diseases such as Fabry disease, cystic fibrosis, α1-antitrypsin deficiency (43–46), and might also hold promise for PH1, where they could prevent AGT aggregation and decrease degradation, thereby increasing the overall level of expression. Agents that increase the affinity of the cofactor would also increase the holo/apo AGT ratio and would be likely to be therapeutically effective on mutants similar to AGT-152. However, merely increasing the proportion of ultimately correctly folded protein may not be enough if the protein can still be targeted to the wrong intracellular compartment, which could be the case for AGT mutants on the minor allele background. The design and testing of therapeutic drugs in PH1 should therefore also include more sophisticated methods such as an assessment of the correct intracellular targeting.

REFERENCES

1. Purdue, P. E., Takada, Y., and Danpure, C. J. (1990) Identification of mutations associated with peroxisome-to-mitochondrion mistargeting of alanine/glyoxylate aminotransferase in primary hyperoxaluria type 1. *J. Cell Biol.* **111,** 2341–2351
2. Purdue, P. E., Allsop, J., Isaya, G., Rosenberg, L. E., and Danpure, C. J. (1991) Mistargeting of peroxisomal L-alanine:glyoxylate aminotransferase to mitochondria in primary hyperoxaluria patients depends upon activation of a cryptic mitochondrial targeting sequence by a point mutation. *Proc. Natl. Acad. Sci. U.S.A.* **88,** 10900–10904
3. Abe, Y., Shodai, T., Muto, T., Mihara, K., Torii, H., Nishikawa, S., Endo, T., and Kohda, D. (2000) Structural basis of presequence recognition by the mitochondrial protein import receptor Tom20. *Cell* **100,** 551–560
4. Obita, T., Muto, T., Endo, T., and Kohda, D. (2003) Peptide library approach with a disulfide tether to refine the Tom20 recognition motif in mitochondrial presequences. *J. Mol. Biol.* **328,** 495–504
5. Danpure, C. J. (2006) Primary hyperoxaluria type 1: AGT mistargeting highlights the fundamental differences between the peroxisomal and mitochondrial protein import pathways. *Biochim. Biophys. Acta* **1763,** 1776–1784
6. Zhang, X., Roe, S. M., Hou, Y., Bartlam, M., Rao, Z., Pearl, L. H., and Danpure, C. J. (2003) Crystal structure of alanine:glyoxylate aminotransferase and the relationship between genotype and enzymatic phenotype in primary hyperoxaluria type 1. *J. Mol. Biol.* **331,** 643–652
7. Eilers, M., and Schatz, G. (1988) Protein unfolding and the energetics of protein translocation across biological membranes. *Cell* **52,** 481–483
8. Leiper, J. M., Oatey, P. B., and Danpure, C. J. (1996) Inhibition of alanine:glyoxylate aminotransferase 1 dimerization is a prerequisite for its peroxisome-to-mitochondrion mistargeting in primary hyperoxaluria type 1. *J. Cell Biol.* **135,** 939–951
9. Lumb, M. J., Drake, A. F., and Danpure, C. J. (1999) Effect of N-terminal α-helix formation on the dimerization and intracellular targeting of alanine:glyoxylate aminotransferase. *J. Biol. Chem.* **274,** 20587–20596
10. Lumb, M. J., Birdsey, G. M., and Danpure, C. J. (2003) Correction of an enzyme trafficking defect in hereditary kidney stone disease *in vitro*. *Biochem. J.* **374,** 79–87
11. Danpure, C. J., Cooper, P. J., Wise, P. J., and Jennings, P. R. (1989) An enzyme trafficking defect in two patients with primary hyperoxaluria type 1: peroxisomal alanine/glyoxylate aminotransferase rerouted to mitochondria. *J. Cell Biol.* **108,** 1345–1352
12. Danpure, C. J. (2001) Primary hyperoxaluria in *The Metabolic and Molecular Bases of Inherited Disease* (Scriver, C. R., Beaudet, A. L., Sly, W. S., and Valle, D., eds), 7th Ed, pp. 3323–3367, McGraw-Hill, New York
13. Motley, A., Lumb, M. J., Oatey, P. B., Jennings, P. R., De Zoysa, P. A., Wanders, R. J., Tabak, H. F., and Danpure, C. J. (1995) Mammalian alanine/glyoxylate aminotransferase 1 is imported into peroxisomes via the PTS1 translocation pathway. Increased degeneracy and context specificity of the mammalian PTS1 motif and implications for the peroxisome-to-mitochondrion mistargeting of AGT in primary hyperoxaluria type 1. *J. Cell Biol.* **131,** 95–109
14. Danpure, C. J., and Jennings, P. R. (1986) Peroxisomal alanine:glyoxylate aminotransferase deficiency in primary hyperoxaluria type I. *FEBS Lett.* **201,** 20–24
15. Purdue, P. E., Lumb, M. J., Allsop, J., Minatogawa, Y., and Danpure, C. J. (1992) A glycine-to-glutamate substitution abolishes alanine:glyoxylate aminotransferase catalytic activity in a subset of patients with primary hyperoxaluria type 1. *Genomics* **13,** 215–218
16. Santana, A., Salido, E., Torres, A., and Shapiro, L. J. (2003) Primary hyperoxaluria type 1 in the Canary Islands: a conformational disease due to I244T mutation in the P11L-containing alanine:glyoxylate aminotransferase. *Proc. Natl. Acad. Sci. U.S.A.* **100,** 7277–7282
17. Danpure, C. J., Purdue, P. E., Fryer, P., Griffiths, S., Allsop, J., Lumb, M. J., Guttridge, K. M., Jennings, P. R., Scheinman, J. I., and Mauer, S. M. (1993) Enzymological and mutational analysis of a complex primary hyperoxaluria type 1 phenotype involving alanine:glyoxylate aminotransferase peroxisome-to-mitochondrion mistargeting and intraperoxisomal aggregation. *Am. J. Hum. Genet.* **53,** 417–432
18. Lumb, M. J., and Danpure, C. J. (2000) Functional synergism between the most common polymorphism in human alanine:glyoxylate aminotransferase and four of the most common disease-causing mutations. *J. Biol. Chem.* **275,** 36415–36422
19. Hopper, E. D., Pittman, A. M., Fitzgerald, M. C., and Tucker, C. L. (2008) *In vivo* and *in vitro* examination of stability of primary hyperoxaluria-associated human alanine:glyoxylate aminotransferase. *J. Biol. Chem.* **283,** 30493–30502
20. Cellini, B., Lorenzetto, A., Montioli, R., Oppici, E., and Voltattorni, C. B. (2010) Human liver peroxisomal alanine:glyoxylate aminotransferase: Different stability under chemical stress of the major allele, the minor allele, and its pathogenic G170R variant. *Biochimie* **92,** 1801–1811
21. Cellini, B., Montioli, R., Paiardini, A., Lorenzetto, A., Maset, F., Bellini, T., Oppici, E., and Voltattorni, C. B. (2010) Molecular defects of the glycine 41 variants of alanine glyoxylate aminotransferase associated with primary

hyperoxaluria type I. *Proc. Natl. Acad. Sci. U.S.A.* **107,** 2896–2901
22. van Woerden, C. S., Groothoff, J. W., Wijburg, F. A., Annink, C., Wanders, R. J., and Waterham, H. R. (2004) Clinical implications of mutation analysis in primary hyperoxaluria type 1. *Kidney Int.* **66,** 746–752
23. Williams, E., and Rumsby, G. (2007) Selected exonic sequencing of the AGXT gene provides a genetic diagnosis in 50% of patients with primary hyperoxaluria type 1. *Clin. Chem.* **53,** 1216–1221
24. Coulter-Mackie, M. B., Lian, Q., Applegarth, D. A., Toone, J., Waters, P. J., and Vallance, H. (2008) Mutation-based diagnostic testing for primary hyperoxaluria type 1: survey of results. *Clin. Biochem.* **41,** 598–602
25. Harambat, J., Fargue, S., Acquaviva, C., Gagnadoux, M. F., Janssen, F., Liutkus, A., Mourani, C., Macher, M. A., Abramowicz, D., Legendre, C., Durrbach, A., Tsimaratos, M., Nivet, H., Girardin, E., Schott, A. M., Rolland, M. O., and Cochat, P. (2010) Genotype-phenotype correlation in primary hyperoxaluria type 1: the p.G170R AGXT mutation is associated with a better outcome. *Kidney Int.* **77,** 443–449
26. Knott, T. G., Birdsey, G. M., Sinclair, K. E., Gallagher, I. M., Purdue, P. E., and Danpure, C. J. (2000) The peroxisomal targeting sequence type 1 receptor, Pex5p, and the peroxisomal import efficiency of alanine:glyoxylate aminotransferase. *Biochem. J.* **352,** 409–418
27. Behnam, J. T., Williams, E. L., Brink, S., Rumsby, G., and Danpure, C. J. (2006) Reconstruction of human hepatocyte glyoxylate metabolic pathways in stably transformed Chinese-hamster ovary cells. *Biochem. J.* **394,** 409–416
28. Oatey, P. B., Lumb, M. J., and Danpure, C. J. (1996) Molecular basis of the variable mitochondrial and peroxisomal localisation of alanine-glyoxylate aminotransferase. *Eur. J. Biochem.* **241,** 374–385
29. Montioli, R., Fargue, S., Lewin, J., Zamparelli, C., Danpure, C. J., Borri Voltattorni, C., and Cellini, B. (2012) The N-terminal extension is essential for the formation of the active dimeric structure of liver peroxisomal alanine:glyoxylate aminotransferase. *Int. J. Biochem. Cell Biol.* **44,** 536–546
30. Bolte, S., and Cordelières, F. P. (2006) A guided tour into subcellular colocalization analysis in light microscopy. *J. Microsc.* **224,** 213–232
31. Rumsby, G., Weir, T., and Samuell, C. T. (1997) A semiautomated alanine: glyoxylate aminotransferase assay for the tissue diagnosis of primary hyperoxaluria type 1. *Ann. Clin. Biochem.* **34,** 400–404
32. Tarn, A. C., von Schnakenburg, C., and Rumsby, G. (1997) Primary hyperoxaluria type 1: diagnostic relevance of mutations and polymorphisms in the alanine:glyoxylate aminotransferase gene (AGXT). *J. Inherit. Metab. Dis.* **20,** 689–696
33. Djordjevic, S., Zhang, X., Bartlam, M., Ye, S., Rao, Z., and Danpure, C. J. (2010) Structural implications of a G170R mutation of alanine:glyoxylate aminotransferase that is associated with peroxisome-to-mitochondrion mistargeting. *Acta Crystallogr. Sect. F Struct. Biol. Cryst. Commun.* **66,** 233–236
34. Cellini, B., Montioli, R., Paiardini, A., Lorenzetto, A., and Voltattorni, C. B. (2009) Molecular insight into the synergism between the minor allele of human liver peroxisomal alanine:glyoxylate aminotransferase and the F152I mutation. *J. Biol. Chem.* **284,** 8349–8358
35. Elgersma, Y., van Roermund, C. W., Wanders, R. J., and Tabak, H. F. (1995) Peroxisomal and mitochondrial carnitine acetyltransferases of *Saccharomyces cerevisiae* are encoded by a single gene. *EMBO J.* **14,** 3472–3479
36. Lee, J. G., Cho, S. P., Lee, H. S., Lee, C. H., Bae, K. S., and Maeng, P. J. (2000) Identification of a cryptic N-terminal signal in Saccharomyces cerevisiae peroxisomal citrate synthase that functions in both peroxisomal and mitochondrial targeting. *J. Biochem.* **128,** 1059–1072
37. Petrova, V. Y., Drescher, D., Kujumdzieva, A. V., and Schmitt, M. J. (2004) Dual targeting of yeast catalase A to peroxisomes and mitochondria. *Biochem. J.* **380,** 393–400
38. Knox, C., Sass, E., Neupert, W., and Pines, O. (1998) Import into mitochondria, folding and retrograde movement of fumarase in yeast. *J. Biol. Chem.* **273,** 25587–25593
39. Sass, E., Karniely, S., and Pines, O. (2003) Folding of fumarase during mitochondrial import determines its dual targeting in yeast. *J. Biol. Chem.* **278,** 45109–45116
40. Strobel, G., Zollner, A., Angermayr, M., and Bandlow, W. (2002) Competition of spontaneous protein folding and mitochondrial import causes dual subcellular location of major adenylate kinase. *Mol. Biol. Cell* **13,** 1439–1448
41. Coulter-Mackie, M. B., and Lian, Q. (2006) Consequences of missense mutations for dimerization and turnover of alanine:glyoxylate aminotransferase: study of a spectrum of mutations. *Mol. Genet. Metab.* **89,** 349–359
42. Walton, P. A., Hill, P. E., and Subramani, S. (1995) Import of stably folded proteins into peroxisomes. *Mol. Biol. Cell* **6,** 675–683
43. Burrows, J. A., Willis, L. K., and Perlmutter, D. H. (2000) Chemical chaperones mediate increased secretion of mutant α1-antitrypsin (α1-AT) Z: A potential pharmacological strategy for prevention of liver injury and emphysema in α1-AT deficiency. *Proc. Natl. Acad. Sci. U.S.A.* **97,** 1796–1801
44. Wang, Y., Loo, T. W., Bartlett, M. C., and Clarke, D. M. (2007) Additive effect of multiple pharmacological chaperones on maturation of CFTR processing mutants. *Biochem. J.* **406,** 257–263
45. Siekierska, A., De Baets, G., Reumers, J., Gallardo, R., Rudyak, S., Broersen, K., Couceiro, J., Van Durme, J., Schymkowitz, J., and Rousseau, F. (2012) α-Galactosidase aggregation is a determinant of pharmacological chaperone efficacy on Fabry disease mutants. *J. Biol. Chem.* **287,** 28386–28397
46. Fan, J. Q., and Ishii, S. (2007) Active-site-specific chaperone therapy for Fabry disease. *FEBS J.* **274,** 4962–4971
47. Danpure, C. J. (1993) Primary hyperoxaluria type 1 and peroxisome-to-mitochondrion mistargeting of alanine:glyoxylate aminotransferase. *Biochimie* **75,** 309–315
48. Coulter-Mackie, M. B., Lian, Q., and Wong, S. G. (2005) Overexpression of human alanine:glyoxylate aminotransferase in *Escherichia coli*: renaturation from guanidine-HCl and affinity for pyridoxal phosphate co-factor. *Protein Expr. Purif.* **41,** 18–26
49. Monico, C. G., Olson, J. B., and Milliner, D. S. (2005) Implications of genotype and enzyme phenotype in pyridoxine response of patients with type I primary hyperoxaluria. *Am. J. Nephrol.* **25,** 183–188
50. Cellini, B., Bertoldi, M., Montioli, R., Paiardini, A., and Borri Voltattorni C. (2007) Human wild-type alanine:glyoxylate aminotransferase and its naturally occurring G82E variant: functional properties and physiological implications. *Biochem. J.* **408,** 39–50